COMPARISON OF ERROR PROPAGATION IN BLOCK ORIENTATION: AN ANALYTICAL APPROACH

J. Cothren [a, *], B. Schaffrin[b]

[a]Department of Geosciences, University of Arkansas, Fayetteville, AR – jcothren@cast.uark.edu
[b]School of Earth Sciences, Ohio State University, Columbus, OH – schaffrin.1@osu.edu

KEY WORDS: Model, Orientation, Integration, Triangulation, Adjustment

ABSTRACT:

Many researchers have reported comparisons between the error propagation properties of direct orientation and indirect orientation (aerial triangulation using ground control points). The results of these comparisons have shown that direct orientation has the potential for use in projects requiring all but the highest accuracy. However, all of these empirical comparisons are specific to the particular configuration of the image block and sensor systems and do not provide an explicit analytical comparison of the general case. In this paper, we present an analytical comparison of the ground point precision obtained from direct and indirect orientation methods within the framework of a block-bundle adjustment in a stochastically constrained Gauss-Markov Model.

1. INTRODUCTION

Accurate and reliable sensor orientation is a pre-requisite for virtually all digital photogrammetric products including georeferenced orthoimages, digital terrain models and (increasingly common) three-dimensional models of man-made surface features. Until very recently analytical aerial triangulation (AT) was the most common method of sensor orientation. Modern methods of AT rely upon the bundle block adjustment, in which possibly large numbers of tie points are – often automatically via correlation or least-squares matching – measured across two or more images and used to estimate the six orientation parameters of each image in the block. Ground control points are integrated into the adjustment as weighted observations and provide datum information to accurately geo-reference the block. As Heipke et al. (2002) and others have remarked, AT is particularly advantageous because the control information resides near the ground features of interest and is therefore largely an interpolation problem. Exterior orientation parameters can be considered nuisance parameters. In fact, AT is often considered a ground control densification process**.

Not long after the Global Positioning System became operational, differential positioning technologies enabled the direct observation of camera exposure centers. The flexible bundle adjustment allowed these additional observations to be seamlessly integrated as weighted observations into the AT solution. This reduced, but did not eliminate, the need for ground control points for datum definition*** and georeferencing. However, tie points were still required for the estimation of the rotation matrix from each camera frame to the model frame.

In the late 1990's, Inertial Measurement Systems (IMU's) made it possible to directly observe a sensor's orientation relative to the ground. Direct observation of the exterior orientation using integrated GPS and IMU systems now allow sensor orientation without manual or automated measurement of either tie points or ground control points – albeit with potential reliability issues because of the lack of redundancy. Many of the original researchers – among them Skaloud and Schwarz (1998), Toth (1998), Burman (1999), Colomina (1999), Grejner-Brzezinska (1999), and Cramer et al. (2000) – demonstrated ground accuracies at the decimeter level without ground control. However, unlike AT solutions in which ground control points provided georeferencing information, these solutions involved extrapolation of control at the sensor to the ground. Furthermore, because the orientation parameters were no longer nuisance parameters, their correlation with each other and fixed interior orientation parameters could not be used advantageously by the adjustment to compensate for poor or variable calibration.

The extrapolation and reliability problems lead to the inclusion of all observations, GPS/IMU, ground control points and tie points into the bundle adjustment in a process popularly known as integrated sensor orientation, or ISO. In particular, as reported by Heipke et al. (2002), ISO may be used to more accurately estimate IMU boresight and GPS phase center offsets in a calibration step, but is also useful in a traditional AT role. In fact, the OEEPE Integrated Sensor Orientation tests (Heipke et al., 2002b) demonstrated mean deviations from independent check points of ± (5-10) cm in planimetry and ± (10-15) cm in height at a 1:5000 image scale. This compared to same-block accuracies from the AT solution of ± (2.0-2.8) cm in planimetry and ±3.2 cm in height. This, and other more recent experiences, clearly demonstrate that direct orientation, while inferior to more labor intensive AT in this case, is sufficient for many lower accuracy projects. At scales of 1:10,000 results showed a similar planimetric accuracy but ±7 cm height accuracy compared to ± (3 – 13.4) cm planimetric accuracy in the direct orientation solution. The wide range of results is due in part to the different system calibration parameters and adjustment coordinate frames.

* Corresponding author

** This was particularly true before widespread use of the bundle adjustment when tie points were used to transfer control throughout the block. Now it is more common to use the exterior orientation estimates produced by the bundle adjustment.

*** Jacobsen and Wegmann (2001) address issues regarding GPS observations in Cartesian frames.

The 2002 OEEPE tests were flown with a dual-frequency GPS receiver and very high quality IMU (Heipke et al., 2002). The tests do not, and were not intended to, shed light on the capability of other integrated sensor systems. With the variety of GPS/IMU configurations available, from low-cost systems to exceedingly capable and expensive systems (cf. Mostafa and Hutton, 2005), the need exists for an analytic relationship among the three orientation solutions – direct orientation, indirect orientation with ground control points, and integrated sensor orientation. The analytic solution should provide insight into the precision required of a pure direct orientation solution (with a boresight-calibrated GPS/IMU system) to achieve ground coordinate precisions equal to a similarly configured indirect AT solution. In this paper we derive inequalities within the framework of a constrained block bundle adjustment. While we do not address ISO explicitly (as did Habib and Schenk, 2002, though using a different approach), the developed framework is suitable for this orientation method as well. Section 2 describes the partitioned bundle block model constrained by pseudo-observations on the parameters (also known as "stochastic constraints"). Section 3 describes how orientation constraints enter the normal equations and affect parameter estimates. These results are then demonstrated at different image scales in Section 4 using a simulated numerical example. We discuss possible extensions to the analytical relationships in Section 5.

2. THE PARTITIONED BUNDLE BLOCK MODEL

The bundle block adjustment is the standard for photogrammetric aerial triangulation because of its comprehensive solution and flexibility. Observations consist of image tie-point measurements, independent ground control point measurements (2 image measurements per point and up to 3 ground coordinate measurements) and the direct observation of exterior orientation parameters with GPS/IMU measurements. If, at first, we only consider observations in the form of image measurements of ground control and tie points, an appropriate stochastic model for the linearized bundle block adjustment (unless additional distortion terms are carried as parameters) is the Gauss-Markov Model (GMM),

$$\mathbf{y} = \mathbf{A}\xi + \mathbf{e}\,, \qquad \mathrm{e} \sim (\mathbf{0}, \sigma_o^2 \mathbf{P}^{-1})\,, \tag{1}$$

in which

- **y** is a *n x 1* random vector of incremental changes to image coordinate observations,
- **A** is an *n x m* non-random design matrix of rank *q = m - 7*, representing the Jacobian matrix of the observation equations with respect to the unknown parameters thereby defining a local differential relationship between parameters and observations,
- ξ is the *m x 1* non-random incremental parameter vector of the linearized observation equations and
- **e** is the *n x 1* random error vector with first and second moments given. The weight matrix **P** is usually treated as a known value (typically it is assumed to be the identity matrix unless image point measurements are of different precision), and the variance component (or reference variance) σ_o^2 is considered as the scale factor for the variance of the image point measurements. If σ_o^2 is chosen to be 1 a priori, then the full observation covariance information is contained in $\mathbf{P}^{-1}$.

Note that in the absence of geo-referencing information from ground control points (i.e. indirect orientation) or direct observations of exterior orientation (i.e. direct orientation), **A** is rank-deficient and the multiple solutions for ξ represent the multiple coordinate frames in which the block can be positioned.

To reduce the computational requirements for solving large photogrammetric blocks, it is common practice to partition design matrices to achieve a particular sparse block-diagonal configuration (cf. Kraus, 1993). We follow this practice because it will later facilitate comparison between direct and indirect orientation, and partition the Gauss-Markov Model as follows:

$$\mathbf{y} = \mathbf{A}_1\xi_1 + \mathbf{A}_2\xi_2 + \mathbf{A}_3\xi_3 + \mathbf{e} \quad , \quad \mathbf{e} \sim (\mathbf{0}, \sigma_o^2 \mathbf{P}^{-1})\,, \tag{2}$$

in which

- $\mathbf{A}_1$ is a *n x* (*6 * number of photos*) matrix containing partial derivatives with respect to the exterior orientation parameters, and ξ_1 contains the incremental changes to the initial approximations of exterior orientation parameters;
- $\mathbf{A}_2$ is a *n* x (*3 * number of gcp points*) matrix containing partial derivatives with respect to the three coordinates (X,Y,Z) of the potential ground control points, and ξ_2 contains the incremental changes to the initial approximations of ground coordinates;
- $\mathbf{A}_3$ is a *n* x (*3 * number of tie points*) matrix containing the partial derivatives of the image coordinate observations with respect to the three ground coordinates of the tie points, and ξ_3 contains the incremental changes to the initial approximations of tie-point ground coordinates. Check points could be incorporated into this partition as well.

Absolute orientation information may enter the model through stochastic constraints on ξ_1 (direct orientation), ξ_2 (indirect orientation), or both. The stochastic constraints required for direct orientation:

$$\mathbf{z}_1 = \xi_1 + \mathbf{e}_1 \qquad \mathbf{e}_1 \sim \left(\mathbf{0}, \sigma_o^2 \mathbf{P}_1^{-1}\right), \tag{3}$$

provide additional information about the exterior orientation elements. Note that we use the same variance component as in (2) which may, for $\sigma_o^2 = 1$, imply that the full GPS/IMU observation covariance is contained in $\mathbf{P}_1^{-1}$. Likewise the stochastic constraints required by indirect orientation (observation of ground control points):

$$\mathbf{z}_2 = \xi_2 + \mathbf{e}_2 \qquad \mathbf{e}_2 \sim \left(\mathbf{0}, \sigma_o^2 \mathbf{P}_2^{-1}\right), \tag{4}$$

provide additional information about ground control point coordinates in ξ_2.

Since the quality of the triangulation is evaluated by the precision (and accuracy) of points on the ground, one measure of the relative quality achieved by each orientation method may be evaluated by the post-adjustment covariance matrix, $\mathbf{Q}_3$, of the estimated tie-point coordinates in ξ_3. In the next section we explicitly express this covariance matrix in terms of both $\mathbf{P}_1$ and $\mathbf{P}_2$. We assume that tie points are measured automatically in the

direct method (but with no control points measured) and in the indirect method (with measured control points). $\mathbf{A}_2$ and $\mathbf{A}_3$ are therefore invariant with respect to the method of georeferencing (and thus to the added stochastic constraints). Furthermore, in the direct method, the ground coordinate parameters contained in ξ_2 are treated as unknowns (i.e. as tie points).

3. CONSTRAINED NORMAL EQUATIONS OF THE PARTITIONED MODEL

The partitioned rank-deficient normal equations for (2) are obtained as

$$\begin{bmatrix} \mathbf{N}_{11} & \mathbf{N}_{12} & \mathbf{N}_{13} \\ \mathbf{N}_{21} & \mathbf{N}_{22} & \mathbf{0} \\ \mathbf{N}_{31} & \mathbf{0} & \mathbf{N}_{33} \end{bmatrix} \begin{bmatrix} \hat{\boldsymbol{\xi}}_1 \\ \hat{\boldsymbol{\xi}}_2 \\ \hat{\boldsymbol{\xi}}_3 \end{bmatrix} = \begin{bmatrix} \mathbf{c}_1 \\ \mathbf{c}_2 \\ \mathbf{c}_3 \end{bmatrix} \tag{5}$$

with $\left[\mathbf{N}_{ij}, \mathbf{c}_i\right] = \mathbf{A}_i^T \mathbf{P}\left[\mathbf{A}_j^T, \mathbf{y}\right]$, and may be augmented with (3) to provide absolute orientation information through direct orientation

$$\begin{bmatrix} \mathbf{N}_{11}+\mathbf{P}_1 & \mathbf{N}_{12} & \mathbf{N}_{13} \\ \mathbf{N}_{21} & \mathbf{N}_{22} & \mathbf{0} \\ \mathbf{N}_{31} & 0 & \mathbf{N}_{33} \end{bmatrix} \begin{bmatrix} \hat{\boldsymbol{\xi}}_1 \\ \hat{\boldsymbol{\xi}}_2 \\ \hat{\boldsymbol{\xi}}_3 \end{bmatrix} = \begin{bmatrix} \mathbf{c}_1+\mathbf{P}_1\mathbf{z}_1 \\ \mathbf{c}_2 \\ \mathbf{c}_3 \end{bmatrix}, \tag{6}$$

or augmented with (4) to provide absolute orientation information via indirect orientation

$$\begin{bmatrix} \mathbf{N}_{11} & \mathbf{N}_{12} & \mathbf{N}_{13} \\ \mathbf{N}_{21} & \mathbf{N}_{22}+\mathbf{P}_2 & \mathbf{0} \\ \mathbf{N}_{31} & \mathbf{0} & \mathbf{N}_{33} \end{bmatrix} \begin{bmatrix} \hat{\boldsymbol{\xi}}_1 \\ \hat{\boldsymbol{\xi}}_2 \\ \hat{\boldsymbol{\xi}}_3 \end{bmatrix} = \begin{bmatrix} \mathbf{c}_1 \\ \mathbf{c}_2+\mathbf{P}_2\mathbf{z}_2 \\ \mathbf{c}_3 \end{bmatrix} \tag{7}$$

Note that the zero blocks in the normal equations (5)-(7) indicate that no observation equations contain both tie and control point coordinates. This is strictly true only in the absence of additional observations in the form of, for example, known distances between a tie and control point. In both cases the addition of sufficient stochastic constraints resolves the rank-deficiency of the normal equations in (5). However, the precision with which the coordinate estimates of the tie-points, $\hat{\boldsymbol{\xi}}_3$, are determined depends upon the structure of the normal equations. Again, since we are concerned with the precision of the ground coordinates in the triangulation, we will examine the effects of (6) versus (7) on the dispersion of $\hat{\boldsymbol{\xi}}_3$. The covariance matrix (or cofactor matrix, if we do not use the a-priori value for the variance component) of all adjusted parameters is contained in a generalized inverse of the normal equations matrix. It can be shown that a reflexive, symmetric generalized inverse of the normal matrix in (5) is given by

$$\begin{bmatrix} \mathbf{N}_{11} & \mathbf{N}_{12} & \mathbf{N}_{13} \\ \mathbf{N}_{21} & \mathbf{N}_{22} & \mathbf{0} \\ \mathbf{N}_{31} & \mathbf{0} & \mathbf{N}_{33} \end{bmatrix}^- = \begin{bmatrix} \mathbf{S}^- & -\mathbf{S}^-\mathbf{N}_{12}\mathbf{N}_{22}^{-1} & -\mathbf{S}^-\mathbf{N}_{13}\mathbf{N}_{33}^{-1} \\ -\mathbf{N}_{22}^{-1}\mathbf{N}_{21}\mathbf{S}^- & \mathbf{N}_{22}^{-1}+\mathbf{N}_{22}^{-1}\mathbf{N}_{21}\mathbf{S}^-\mathbf{N}_{12}\mathbf{N}_{22}^{-1} & \mathbf{N}_{22}^{-1}\mathbf{N}_{21}\mathbf{S}^-\mathbf{N}_{13}\mathbf{N}_{33}^{-1} \\ -\mathbf{N}_{33}^{-1}\mathbf{N}_{31}\mathbf{S}^- & \mathbf{N}_{33}^{-1}\mathbf{N}_{31}\mathbf{S}^-\mathbf{N}_{12}\mathbf{N}_{22}^{-1} & \mathbf{N}_{33}^{-1}+\mathbf{N}_{33}^{-1}\mathbf{N}_{31}\mathbf{S}^-\mathbf{N}_{13}\mathbf{N}_{33}^{-1} \end{bmatrix} \tag{8}$$

with $\mathbf{S} = \mathbf{N}_{11} - \mathbf{N}_{12}\mathbf{N}_{22}^{-1}\mathbf{N}_{21} - \mathbf{N}_{13}\mathbf{N}_{33}^{-1}\mathbf{N}_{31}$. Here $\mathbf{S}^-$ denotes any reflexive, symmetric g-inverse of $\mathbf{S}$ (Magnus and Neudecker, 1999, pg. 12). The lower right block is the covariance matrix of the tie-point coordinate estimates and, thus, the matrix that the users would like to see minimized. The pseudo-observations, whether from direct or indirect information, affect $\mathbf{Q}_3$ through $\mathbf{S}$. If geo-referencing information is provided directly through calibrated GPS/IMU observations, the pseudo-observations in (6) create the, now full-rank, matrix

$$\mathbf{S}_1 = \mathbf{N}_{11} + \mathbf{P}_1^{-1} - \mathbf{N}_{12}\mathbf{N}_{22}^{-1}\mathbf{N}_{21} - \mathbf{N}_{13}\mathbf{N}_{33}^{-1}\mathbf{N}_{31} \tag{9}$$

instead of $\mathbf{S}$, and we may write the tie-point cofactor matrix in terms of the inverse of $\mathbf{S}_1$ as

$$\mathbf{Q}_3^{(1)} = \mathbf{N}_{33}^{-1} + \mathbf{N}_{33}^{-1}\mathbf{N}_{31}\mathbf{S}_1^{-1}\mathbf{N}_{13}\mathbf{N}_{33}^{-1}. \tag{10}$$

The superscript $^{(1)}$ is used to indicate that the tie point coordinate estimates are obtained via the direct method. Alternatively, if the georeferencing information is provided indirectly, through ground control points only, the pseudo-observations in (7) create the full-rank matrix

$$\mathbf{S}_2 = \mathbf{N}_{11} - \mathbf{N}_{12}\left(\mathbf{N}_{22}+\mathbf{P}_2\right)^{-1}\mathbf{N}_{21} - \mathbf{N}_{13}\mathbf{N}_{33}^{-1}\mathbf{N}_{31}. \tag{11}$$

The covariance matrix of the tie-point coordinates achieved through indirect orientation may thus be written as

$$\mathbf{Q}_3^{(2)} = \mathbf{N}_{33}^{-1} + \mathbf{N}_{33}^{-1}\mathbf{N}_{31}\mathbf{S}_2^{-1}\mathbf{N}_{13}\mathbf{N}_{33}^{-1} \tag{12}$$

In this case the superscript $^{(2)}$ indicates that the estimates were obtained via the indirect method. Now we are ready to analytically relate the tie-point precision to the orientation information contained in $\mathbf{P_1}$ or $\mathbf{P_2}$, respectively. If $\mathbf{Q}_3^{(1)} \le \mathbf{Q}_3^{(2)}$, then direct orientation leads to a better tie-point precision than indirect orientation; for details of this comparison see Marshall and Olkin (1979). From (10) and (12) we see that this inequality holds *if and only if* $\mathbf{S_1} \ge \mathbf{S_2}$. This is to be expected since from (8) we know that the inverses of $\mathbf{S_1}$ and $\mathbf{S_2}$ are the respective covariance matrices of the exterior orientation elements if constrained by direct and indirect observations, respectively. By substituting (9) and (11) into this inequality it can be shown (see Appendix A for details) that

$$\mathbf{Q}_3^{(1)} \le \mathbf{Q}_3^{(2)} \Leftrightarrow \mathbf{P}_1 \ge \mathbf{N}_{12}\mathbf{N}_{22}^{-1}\left(\mathbf{N}_{22}^{-1}+\mathbf{P}_2^{-1}\right)^{-1}\mathbf{N}_{22}^{-1}\mathbf{N}_{21}. \tag{13}$$

This expression provides us with a measure to determine the weight matrix (or the covariance matrix) of the direct stochastic constraints that is required to achieve, at least, the same precision as an indirect adjustment with a given ground control

configuration (which is contained in $\mathbf{N}_{22}$ and $\mathbf{N}_{12}$) and precision (contained in $\mathbf{P}_2$). Continued manipulation of (13) can likewise isolate $\mathbf{P}_2$, leading to the equivalence

$$\mathbf{Q}_3^{(1)} \le \mathbf{Q}_3^{(2)} \Leftrightarrow$$

$$\mathbf{P}_2 \le \mathbf{N}_{22}\left(\begin{array}{c}\mathbf{N}_{21}\mathbf{N}_{11}^{-1}\mathbf{N}_{12}\left(\mathbf{N}_{21}\mathbf{N}_{11}^{-1}\mathbf{P}_1\mathbf{N}_{11}^{-1}\mathbf{N}_{21}\right)^{-1}\cdot \\ \cdot\ \mathbf{N}_{21}\mathbf{N}_{11}^{-1}\mathbf{N}_{21}-\mathbf{N}_{22}\end{array}\right)^{-1}\mathbf{N}_{22} \quad . \qquad (14)$$

The inequalities (13) and (14) are satisfied when direct orientation provides uniformly higher precision estimates of the tie point coordinates. It is important to note that the tie point configuration, which is assumed to be invariant between the two geo-referencing methods, does not affect the comparison. Therefore, these inequalities also hold for any number of tie points included in the adjustment. Furthermore, ground point coordinates computed by intersection apart from the bundle adjustment (as in DEM generation and feature extraction) benefit from the chosen orientation method quite similarly to tie points used in the adjustment. This is true because $\mathbf{S}_1$ and $\mathbf{S}_2$ (the weight matrices of the estimated exterior orientation parameters) are used directly in the estimation of the precision of subsequent ground points. Also, we assume that the image coordinates of the ground control points are included in the adjustment, regardless of the orientation method, and simply serve as additional tie points in the direct method if they appear in multiple images.

More details about the matrix inequalities used throughout the preceding analysis can be found in Appendix B. In the next section we use the key results (13) and (14) in an example involving simulated fifty-six-image aerial blocks at two different scales.

4. COMPARISON IN A SIMULATED BLOCK: AN EXAMPLE

To demonstrate how the analysis above might be practically used, we consider two blocks, each composed of four strips of seven images each. One block is to be acquired at a scale of 1:4,800, the other at a sale of 1:24,000. Details of each block are given in Table 1 and the network configuration is shown in Figure 2. The ground control points for both blocks are assumed to be collected with GPS techniques yielding a horizontal coordinate variance of 0.0025 m^2 and a vertical coordinate variance of 0.0225 m^2 with (assumed) zero correlation among the coordinates. Also, the exposure center coordinates and orientation parameters are assumed to be observed with GPS/IMU devices yielding coordinate variances of 0.01 m^2 in the horizontal and 0.09 m^2 in the vertical, again without correlation. Orientation angles can be observed with a variance of 0.0001 $degrees^2$ in omega and phi, 0.01 $degrees^2$ in kappa with zero correlation. These variances reflect results achieved from calibrated systems (Heipke et al., 2002).

Block	Over –lap (%)	Side-lap (%)	B/H Ratio	Focal Len. (mm)	Format (mm)
1:4,800	60	30 %	1:1.6	150	235 x 235
1:24,000	60	30 %	1:1.6	150	235 x 235

Table 1. Acquisition parameters of the simulated block.

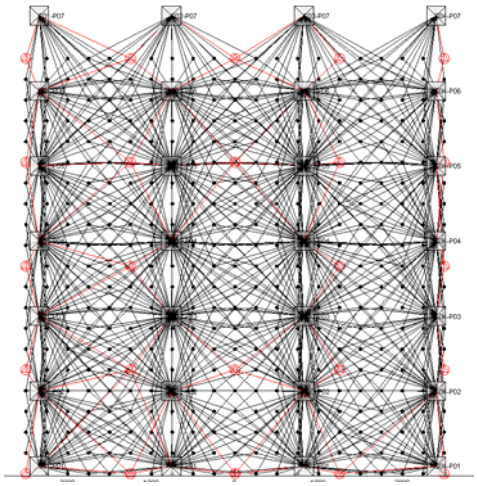

Figure 2. Configuration of the simulated block. Ground points used as control are shown in red.

A simulated trial consists of an aerial image block generated from the "true" values of both exterior orientation and ground points (both tie and control) as follows:

Direct orientation, simulated dataset:

1. Image point coordinates (x,y) are generated by perturbing the "true" values (generated by the collinearity equations using the "true" values of exterior orientation and ground points) with normally distributed random errors with a standard deviation of ±0.005 mm.
2. Initial estimates of the exterior orientation parameters are generated by perturbing the "true" values with normally distributed random errors with a standard deviation consistent with the assumptions in the preceding paragraph.
3. Initial estimates of the ground point coordinates (including ground control points) are intersected using the image coordinates developed in the first step and the exterior orientation values developed in the second step.
4. Pseudo-observations are added to the exterior orientation parameters per equation(3).

Indirect orientation, simulated dataset:

1. Image point coordinates (x,y) are generated as in the direct case.
2. Ground control point coordinates are perturbed with normally distributed random errors with a standard deviation consistent with the assumptions in the preceding paragraph.
3. Initial estimates for the horizontal coordinates of the exposure station are generated by solving a two-dimensional similarity transform between image coordinates and ground control points (2 in each image of the block). Exposure station Z-coordinate is assigned the flying height. The orientation angles phi and omega are assumed to be zero, kappa is assumed zero degrees in strips 1 and 3 and 180 degrees in strips 2 and 4.
4. Initial estimates of the tie points are intersected using the image coordinates developed in step one and the exterior orientation parameters developed in step 3.
5. Pseudo-observations are added to the ground control points per equation (4).

These results show that networks of a larger scale tend to yield comparable accuracies between the two orientation procedures, although horizontal accuracy appears to improve substantially with indirect orientation. The results also confirm our expectations that, as the photo scale decreases, both accuracy and precision are more drastically improved by indirect orientation procedures as compared to direct orientation procedures. Note that in both blocks the difference between the horizontal accuracies is somewhat larger than the difference between the vertical accuracies.

	Direct (±m)	Indirect (±m)	Direct (±m)	Indirect (±m)
Horz RMS	0.18	0.09	0.48	0.16
Total RMS	0.27	0.26	0.69	0.31
$\|\Delta X\|$	0.13	0.06	0.28	0.10
$\|\Delta Y\|$	0.10	0.05	0.33	0.11
$\|\Delta Z\|$	0.23	0.17	0.43	0.24
$3\sigma_X$	0.33	0.21	1.03	0.49
$3\sigma_Y$	0.33	0.21	1.12	0.47
$3\sigma_Z$	0.68	0.61	1.70	1.16

Table 3. Mean tie point coordinate results of 100 trials. RMS values compare estimated tie point coordinates with their "true" values. Sigma values are derived from variances propagated through the orientation adjustment.

From the point of view of the network designer, equation (13) is most useful in that it tells what modifications to the direct observations of the exterior orientation parameters are required to achieve the precision of the indirect method. We, therefore, consider the normal equations formed from the "design" values of the tie points, ground control points, and exterior orientation used to generate the simulations. The matrix norms of the partitioned normal equations and pseudo-observation weight matrices are shown in Table 3. Note that from these measurements we may determine the decrease of variance of each parameter estimate (the entries in the diagonal matrix $\mathbf{P}_1$) required to achieve precisions equal to orientation with ground control points with variances reflected in $\mathbf{P}_2$. According to row 3 in Table 3, the exterior orientation parameters would have to be observed with, on average, 1.9 times higher precision in the 1:4,800 scale block, and with 5.4 times higher precision in the 1:24,000 scale block.

Although each trial is developed from the same true values, each is unique due to the added random perturbations. Both the direct and indirect trials are consistent with standard operational procedures for providing initial approximations. The mean results of 100 trials are detailed in Table 3. All RMS values are considered accuracy measures in that they show mean deviations from the "true" values. The sigma values are propagated errors form the orientation procedures.

Partitioned matrices (eq.14)	Frobenius Norm 1:4,800	Frobenius Norm 1:24,000
$\mathbf{P_1}$	92.8×10^6	92.8×10^6
Eq. 13	338.0×10^6	2688.0×10^6
$\mathbf{P_2}$	283	283
Eq. 14	4690	493

Table 4. Matrix norms of the partitioned matrices.

	1:4,800	1:24,000
Frobenius Norm P_1	9.2×10^7	9.2×10^7
Frobenius Norm RHS (14)	3.37×10^8	2.687×10^9
P_1 scaling required	3.640	28.945
Direct Observation Variance Decrease Factor	0.275	0.0345

Table 5. Scaling of the weight matrix for direct orientation required to achieve a precision equal to the indirect method

5. CONCLUSIONS AND OUTLOOK

The framework developed in this paper has been used to derive an analytic relationship between two differently constrained bundle adjustments – direct and indirect – and is a step towards a more general method to compare various weighting methods for bundle adjustments. The framework may also be extended to include 1) the ISO method and 2) and integrated LiDAR observations, thereby following similar lines as Burman (2000) and Csanyi and Toth (2007).

REFERENCES

Burman, H., 1999. Using GPS and INS for orientation of aerial photography, *Proceedings of the ISPRS Workshop "Direct versus indirect methods of sensor orientation"*, Barcelona, pp. 148-157.

Burman, H., 2000. Adjustment of laser scanner data for correction of orientation errors. *Intl. Arch. of Photogrammetry and Remote Sensing*, v. 33, Part B3, pp. 125.132.

Caspary, W. F., 1987. *Concepts of Network and Deformation Analysis.* Monograph 11, School of Geomatics Engineering (formerly Surveying), The University of New South Wales, Kensington, NSW, Australia.

Colomina, I., 1999. GPS/INS and Aerial Triangulation: What is the best way for the operational determiniation of photogrammetric image orientation? *Intl. Arch. of Photogrammetry and Remote Sensing*, v. 32, Part 3-2W5, pp. 121.-130.

Cramer, M., Stallmann, D. and Haala, N., 2000. Direct georeferencing using GPS/inertial exterior orientations for photogrammetric applications; *Intl. Arch. of Photogramm. and Remote Sensing*, v. 33, part B3, pp. 198-205.

Csanyi, N., and Toth, C., 2007. Improvement of LiDAR data accuracy using LiDAR specific ground targets. *Photogramm. Engrg. & Remote Sensing*, 73(4), pp. 385-396.

Grejner-Brzezinska, D.A., 1999. Direct Exterior Orientation of Airborne Imagery with GPS/INS System: Performance Analysis. *Navigation*, Vol. 46, No. 4, pp. 261-270.

Grejner-Brzezinska, D.A., 2001. Direct Sensor Orientation in Airborne and Land-based Mapping Applications. *Geodetic & GeoInformation Science Report No. 461.* Department of Civil and Environmental Engineering and Geodetic Science. The Ohio State University, Columbus, OH, USA.

Habib, A., and Schenk, T., 2002. Accuracy analysis of reconstructed points in object space from direct and indirect

exterior orientation methods, In: *OEEPE Official Publ*. No 43, pp. 47-52.

Heipke C., Jacobsen, K., and Wegmann, H, 2002. Analysis of the results of the OEEPE test of Integrated Sensor Orientation. In: *OEEPE Official Publ*. No 43, pp. 31-45.

Jacobsen, K., and Wegmann, H., 2001. Dependencies and problems of direct sensor orientation. In: *OEEPE Official Publ*. No 43, pp. 73-84.

Kraus, K., 1993. *Photogrammetry, Volume 1, Fundamentals and Standard Processes*. Duemmler: Bonn, pp. 279-289.

Magnus, J.R., and Neudecker, H., 1999. *Matrix Differential Calculus with Applications in Statistics and Econometrics*. Wiley: Chichester, pp. 11-12.

Marshall, A.W., and Olkin, I., 1979. Albert W. Marshall, Ingram Olkin, *Inequalities: Theory of Majorization and its Applications*. *Mathematics in Science and Engineering*, Vol. 143, Academic Press, New York, 1979, 569 pages.

Mostafa, M.M.R., and Hutton, J., 2005. A Fully Integrated Solution for Aerial Surveys: Design, Development, and Performance Analysis. *Photogramm. Engrg. & Remote Sensing*, 71(4), pp. 391-398.

Skaloud, J., and Schwartz, K.P., 1998. Accurate orientation for airborne mapping systems. *Intl. Arch. of Photogramm. and Remote Sensing*, v. 32, Part 2, pp. 282-290.

Toth, C., 1998. Direct platform orientation of multi-sensor data acquisition systems. *Intl. Arch. of Photogramm. and Remote Sensing*, v. 32, Part 4, pp. 629-634.

APPENDIX A. DERIVATION OF COVARIANCE RELATIONS

For the direct method to achieve equivalent or better ground point accuracies, $\mathbf{S}_1 \geq \mathbf{S}_2$. Using expressions (13) and (14) then

$$\mathbf{N}_{11} + \mathbf{P}_1 - \mathbf{N}_{12}\mathbf{N}_{22}^{-1}\mathbf{N}_{21} - \mathbf{N}_{13}\mathbf{N}_{33}^{-1}\mathbf{N}_{31} \geq$$
$$\mathbf{N}_{11} - \mathbf{N}_{12}\left(\mathbf{N}_{22} + \mathbf{P}_2\right)^{-1}\mathbf{N}_{21} - \mathbf{N}_{13}\mathbf{N}_{33}^{-1}\mathbf{N}_{31}$$

must hold with respect to the precision of the competing orientation methods. We may obviously eliminate the term containing tie-point information because it is invariant with respect to the orientation method and obtain

$$\mathbf{P}_1 - \mathbf{N}_{12}\mathbf{N}_{22}^{-1}\mathbf{N}_{21} \geq -\mathbf{N}_{12}\left(\mathbf{N}_{22} + \mathbf{P}_2\right)^{-1}\mathbf{N}_{21}$$
$$\mathbf{P}_1 \geq \mathbf{N}_{12}\mathbf{N}_{22}^{-1}\mathbf{N}_{21} - \mathbf{N}_{12}\left(\mathbf{N}_{22} + \mathbf{P}_2\right)^{-1}\mathbf{N}_{21}$$
$$\mathbf{P}_1 \geq \mathbf{N}_{12}\mathbf{N}_{22}^{-1}\mathbf{N}_{21} - \mathbf{N}_{12}\mathbf{N}_{22}^{-1}\mathbf{N}_{21} + \mathbf{N}_{12}\mathbf{N}_{22}^{-1}\left(\mathbf{N}_{22}^{-1} + \mathbf{P}_2^{-1}\right)^{-1}\mathbf{N}_{22}^{-1}\mathbf{N}_{21}$$

$$\mathbf{P}_1 \geq \mathbf{N}_{12}\mathbf{N}_{22}^{-1}\left(\mathbf{N}_{22}^{-1} + \mathbf{P}_2^{-1}\right)^{-1}\mathbf{N}_{22}^{-1}\mathbf{N}_{21}$$
$$\mathbf{P}_1 \geq \mathbf{N}_{12}\mathbf{N}_{22}^{-1}\left(\mathbf{I} + \mathbf{N}_{22}\mathbf{P}_2^{-1}\right)\mathbf{N}_{21}$$
$$\mathbf{P}_1 \geq \mathbf{N}_{12}\left(\mathbf{N}_{22} + \mathbf{N}_{22}\mathbf{P}_2^{-1}\mathbf{N}_{22}\right)^{-1}\mathbf{N}_{21}.$$

If $\mathbf{N}_{21}$ has full-row rank, then we may further rearrange the expression to obtain the following equivalent statements

$$\mathbf{N}_{21}\mathbf{N}_{11}^{-1}\mathbf{P}_1\mathbf{N}_{11}^{-1}\mathbf{N}_{12} \geq \mathbf{N}_{21}\mathbf{N}_{11}^{-1}\mathbf{N}_{12}\left(\mathbf{N}_{22} + \mathbf{N}_{22}\mathbf{P}_2^{-1}\mathbf{N}_{22}\right)^{-1}\mathbf{N}_{21}\mathbf{N}_{11}^{-1}\mathbf{N}_{12}$$
$$\left(\mathbf{N}_{21}\mathbf{N}_{11}^{-1}\mathbf{N}_{12}\right)^{-1}\mathbf{N}_{21}\mathbf{N}_{11}^{-1}\mathbf{P}_1\mathbf{N}_{11}^{-1}\mathbf{N}_{12}\left(\mathbf{N}_{21}\mathbf{N}_{11}^{-1}\mathbf{N}_{12}\right)^{-1} \geq \left(\mathbf{N}_{22} + \mathbf{N}_{22}\mathbf{P}_2^{-1}\mathbf{N}_{22}\right)^{-1}$$
$$\mathbf{N}_{22} + \mathbf{N}_{22}\mathbf{P}_2^{-1}\mathbf{N}_{22} \geq \left(\mathbf{N}_{21}\mathbf{N}_{11}^{-1}\mathbf{N}_{12}\right)\left(\mathbf{N}_{21}\mathbf{N}_{11}^{-1}\mathbf{P}_1\mathbf{N}_{11}^{-1}\mathbf{N}_{12}\right)^{-1}\left(\mathbf{N}_{21}\mathbf{N}_{11}^{-1}\mathbf{N}_{12}\right)$$
$$\mathbf{P}_2^{-1} \geq \left(\mathbf{N}_{22}^{-1}\mathbf{N}_{21}\mathbf{N}_{11}^{-1}\mathbf{N}_{12}\right)\left(\mathbf{N}_{21}\mathbf{N}_{11}^{-1}\mathbf{P}_1\mathbf{N}_{11}^{-1}\mathbf{N}_{12}\right)^{-1}\left(\mathbf{N}_{21}\mathbf{N}_{11}^{-1}\mathbf{N}_{21}\mathbf{N}_{22}^{-1}\right) - \mathbf{N}_{22}^{-1}$$

leading finally to

$$\mathbf{P}_2 \leq \mathbf{N}_{22}\left(\begin{array}{c}\mathbf{N}_{21}\mathbf{N}_{11}^{-1}\mathbf{N}_{12}\left(\mathbf{N}_{21}\mathbf{N}_{11}^{-1}\mathbf{P}_1\mathbf{N}_{11}^{-1}\mathbf{N}_{12}\right)^{-1}\cdot \\ \cdot\ \mathbf{N}_{21}\mathbf{N}_{11}^{-1}\mathbf{N}_{12} - \mathbf{N}_{22}\end{array}\right)^{-1}\mathbf{N}_{22}$$

APPENDIX B. MATRIX NORMS AND LÖWNER'S PARTIAL ORDERING OF MATRICES

Given two matrices of equal size, **G** and **H**, a partial ordering according to Löwner (cf. Marshall and Olkin,1979) can be defined through $\mathbf{G} > \mathbf{H}$ if and only if $\mathbf{G} - \mathbf{H}$ is positive-definite, or slightly more generally, $\mathbf{G} \geq \mathbf{H}$ if and only if $\mathbf{G} - \mathbf{H}$ is positive-semi-definite. In the case that **G** itself is positive-definite and **H** is, at least, positive-semi-definite, we may conclude $\mathbf{G} \geq \mathbf{H}$ if and only if the maximum eigenvalue of the positive-semi-definite matrix $\mathbf{G}^{-1}\mathbf{H}$ is less than one.

A justification for this is related to the relative size of a quadratic function of the two matrices. For details see Caspary (1987). Instead of comparing the matrices themselves, we may compare certain scalar-valued functions of them; for instance, the trace of **G** with the trace of **H**. Another possibility is the (weighted-) Frobenius norm, defined as $\|\mathbf{G}\|_w^2 = tr\left(\mathbf{G}^T\mathbf{W}\mathbf{G}\right)$ for some positive-definite matrix, **W**. For $\mathbf{W} \equiv \mathbf{I}$, this norm is equal to the sum of squared eigenvalues of **G** and can be thought of as a measure of the "hyper-volume" of the positive semi-definite matrix **G**. The weighted Frobenius norm provides a simple composite measure that can be used to scale the norm of **G** to that of **H**. For example, if $\frac{\|\mathbf{G}\|_w}{\|\mathbf{H}\|_w} = r \leq 1$ then by this measure at least, **G** is "smaller" than **H** by a factor of *r*. *r* may be applied as a scale factor to the norm of **G** then, $r\sqrt{tr\left(\mathbf{G}^T\mathbf{G}\right)} = \sqrt{tr\left(r\mathbf{G}^T r\mathbf{G}\right)} = \sqrt{tr\left(\bar{\mathbf{G}}^T\bar{\mathbf{G}}\right)}$ so that the norm of matrix $\bar{\mathbf{G}}$ is now equal to that of **H**.